Molecular Orbital Studies of the Structures and Reactions of a Singly Charged Calcium Ion with Water Clusters, $Ca^+(H_2O)_n$

Hidekazu Watanabe and Suehiro Iwata*

Graduate University for Advanced Studies, Institute for Molecular Science, Myodaiji, Okazaki 444 Japan

Received: June 18, 1996; In Final Form: October 21, 1996[⊗]

Structures of hydrated singly positive charged calcium−water clusters $Ca^+(H_2O)_n$ and their hydrogen-eliminated products $(CaOH)^+(H_2O)_{n-1}$ were optimized using the ab initio molecular orbital methods and are compared with cationic magnesium−water clusters which have been investigated previously. For $n \geq 2$, the structures of $Ca^+(H_2O)_n$ are different from those of $Mg^+(H_2O)_n$. In the $Mg^+(H_2O)_n$ clusters, a pyramidical $Mg^+(H_2O)_3$ forms the first shell. In contrast, a quasi-square-planar $Ca^+(H_2O)_4$ is the first shell. The structures of $(CaOH)^+(H_2O)_{n-1}$ are also different from structures $(MgOH)^+(H_2O)_{n-1}$. The structural difference is attributed to the participation of the d orbitals of Ca atom in the bonding. Despite these structural differences, the core molecular ion $(CaOH)^+$ in the hydrogen-eliminated products $(CaOH)^+(H_2O)_{n-1}$ is very similar to the corresponding core ion $(MgOH)^+$. Both ions, $CaOH^+$ and $MgOH^+$, are strongly polarized to $Ca^{2+}O^-H$ and $Mg^{2+}O^-H$. Consequently, the hydration energies of the $(CaOH)^+(H_2O)_n$ are much larger than those of the corresponding $Ca^+(H_2O)_n$. The internal energy change of the hydrogen-elimination reactions of the $Ca^+(H_2O)_n$ is positive for $n = 1-4$ but becomes negative for $n \geq 5$, which is consistent with the product switch in the time-of-flight mass spectrum reported by Fuke's group. The equilibrium constants of the hydrogen elimination reaction are also consistent with the experimental observed isotope effects and the determined metal dependencies.

1. Introduction

In aqueous solution a salt molecule is dissociated to a cation and an anion surrounded by several water molecules. The hydration stabilizes these ions. Hydrated model ion clusters can be considered as a model of the structures around the ions in aqueous solution.

By development of molecular beam techniques, investigations of hydrated metal clusters becomes possible. Singly charged group 2 metals have one valence electron, and their hydrated clusters are isoelectronic to alkali metal−water clusters. Several spectroscopic studies for $Sr^+(H_2O)_n$, $Ca^+(H_2O)_n$, and $Mg^+(H_2O)_n$[1−11] were reported. From the theoretical side, Bauschlicher and co-workers reported the structures of $Sr^+(H_2O)_n$, $Ca^+(H_2O)_n$, and $Mg^+(H_2O)_n$ ($n \leq 3$)[12−16] using the ab initio molecular orbital methods. We have also investigated the structures of $Mg^+(H_2O)_n$ for larger n and have discussed their stability.[17] Doubly charged group 2 metal−water clusters $M^{2+}(H_2O)_n$ (M = Mg, Ca, Sr, Ba, and Ra) have been studied by Glendening and Feller.[18] Hashimoto et al. analyzed the structures and stabilities of $Be(H_2O)_n$ and $Be^{2+}(H_2O)_n$.[19−21]

Fuke's and also Castleman's groups observed characteristic size distributions in the time-of-flight (TOF) mass spectra of $M^+(H_2O)_n$ and their reaction products (M = Mg and Ca).[3,9,11] Up to about $n = 6$, hydrated clusters $M^+(H_2O)_n$ are the dominant product. On contrary, for the cluster size in the range $6 \leq n \leq 15$, the dominant products are hydrogen eliminated ions $M^+(H_2O)_{n-1}$. Apparently the reaction

$$M^+(H_2O)_n \rightarrow MOH^+(H_2O)_{n-1} + H \qquad (1)$$

takes place in the collision reactions of metal ions with the water clusters. For $n \geq 15$, the dominant product becomes nonreactive $Mg^+(H_2O)_n$ again. Fuke and co-workers called the change of the dominant reactive product at $n = 6$ "the first product switch", and at $n = 15$ "the second product switch". In our previous study,[17] we investigated the structures and stabilities of $Mg^+(H_2O)_n$ and $MgOH^+(H_2O)_{n-1}$. We successfully elucidated the first products switch in this reaction system, which was attributed to the relative thermochemical stabilities. The product, $MgOH^+(H_2O)_{n-1} + H$, became more stable than $Mg^+(H_2O)_n$ for $n = 5$.

In the present work, we investigate the $Ca^+-(H_2O)_n$ reaction system and examine the similarities and differences of the Ca^+ and Mg^+ systems. Among group 2 metals, the first two elements Be and Mg are distinguished from the other elements. The chemistry of beryllium and magnesium is in most cases different from that of the other group 2 elements. Despite the differences, similar trends for the above-mentioned reactions are found in the products of the reactions, $Mg^+ + (H_2O)_n$ and $Ca^+ + (H_2O)_n$.

Kochanski et al. investigated $Ca^+(H_2O)_n$ clusters up to $n = 10$, using the Monte Carlo method.[22] In ab initio molecular orbital calculations, the structures for $n = 1$ and 2 have been already determined by Bauschlicher et al.[13] But no reports with the ab initio molecular orbital methods are presented for the larger size of $Ca^+(H_2O)_n$ clusters. In the present paper, the structures of singly charged calcium−water clusters $Ca^+(H_2O)_n$ and their hydrogen-eliminated clusters $CaOH^+(H_2O)_{n-1}$ up to $n = 8$ are determined using the ab initio molecular orbital methods. The hydration and hydrogen elimination energies are evaluated, and the stabilities of $Ca^+(H_2O)_n$ and $CaOH^+(H_2O)_{n-1}$ are discussed. The thermochemical functions and equilibrium constants are calculated, and the experimental product switches are analyzed.

2. Method

Structures of calcium−water cation clusters, $Ca^+(H_2O)_n$, are optimized with the unrestricted self-consistent field (UHF), and the hydrogen eliminated clusters $(CaOH)^+(H_2O)_{n-1}$ ($n = 1-8$)

* To whom correspondence should be sent.

[⊗] Abstract published in *Advance ACS Abstracts,* January 1, 1997.

S1089-5639(96)01798-7 CCC: $14.00

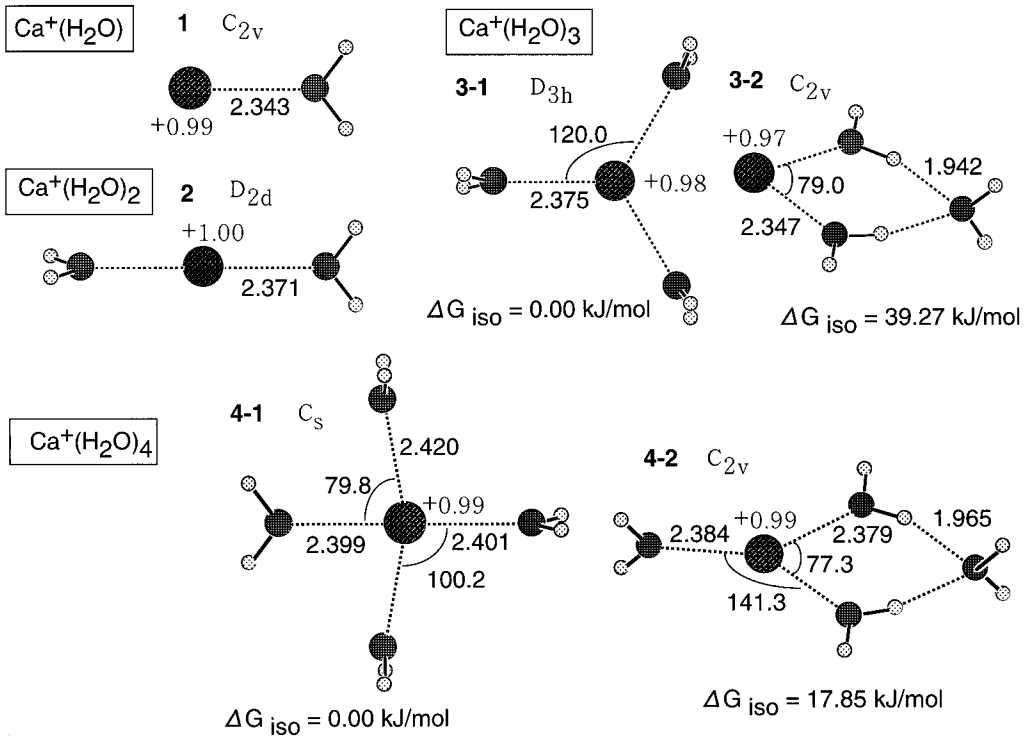

Figure 1. Geometric structures of singly charged hydrated calcium clusters $Ca^+(H_2O)_n$ (for $n \leq 4$). Characteristic geometric parameters and natural charges are written in the figure. Geometric parameters are given in angstroms and degree. Values under structures are Gibbs' free energy change at room temperature (ΔG_{iso}).

are optimized with the restricted self-consistent-field (RHF) method. All the geometric parameters are optimized in this study. To confirm the stationary point, the harmonic frequencies at the optimized structures are evaluated. For calcium, the used basis set is [12s9p5d/9s7p3d] of ref 23 and for oxygen and hydrogen, the 6-31G* basis set was employed. The hydration energies and the hydrogen elimination energies are evaluated within the SCF optimized approximation. For the smaller clusters, we also estimated the reaction energies with the MP2-(all electrons) and MP4SDTQ(all electrons) approximations at the SCF geometries. In all approximations, the hydration and hydrogen-elimination reaction energies were corrected by zero-point vibration energies, at the SCF level of theory. To analyze the experimental isotope effects, we also calculated the zero-point vibration energies of the deuterium water clusters $Ca^+(D_2O)_n$ and $(CaOD)^+(D_2O)_{n-1}$. Moreover, the thermochemical functions and equilibrium constants are evaluated under assumption of an ideal gas.

Programs used for optimization are GAUSSIAN92[24] and GAUSSIAN94.[25] To evaluate thermochemical functions and equilibrium constant, small programs were coded.

3. Results and Discussions

3.1. Structures of Clusters $Ca^+(H_2O)_n$. The geometric structures of $Ca^+(H_2O)_n$ ($n \leq 4$) are shown in Figure 1. Only the characteristic geometric parameters and natural charges are shown in the figure. The detailed parameters will be provided through E-mail[26] on request. Tables 1 and 2 summarize the thermochemical functions for the isomerization and hydration reaction of $Ca^+(H_2O)_n$.

Structure **1** ($Ca^+(H_2O)$) in Figure 1 is a one-to-one complex of a singly charged calcium ion and a water molecule. All four atoms lie in a plane, and the cluster belongs to the C_{2v} point group. In the $Ca^+(H_2O)_2$ cluster, the O−Ca−O frame (structure **2** of Figure 1) is linear, and thus, the cluster has D_{2d} symmetry. The two water molecules of $Ca^+(H_2O)_2$ have a staggered conformation. These structures are in line with investigation of Bauschlicher et al.[13] The collinearity of O−Ca−O is contrasted with an almost right angle of O−Mg−O in $Mg^+(H_2O)_2$. As is compared in Table 2, the water−water interaction energy is much larger than the hydrogen-bonding energy of water dimer.

TABLE 1: Thermochemical Functions for the Isomerization Reaction of $Ca^+(H_2O)_n$[a]

		ΔE_{iso}				
cluster	reaction	without zero-point vib corr	with zero-point vib corr	ΔH_{iso}	ΔS_{iso}	ΔG_{iso}
$Ca^+(H_2O)_3$	**3-1** → **3-2**	26.81	33.96	30.89	−28.09	39.27
$Ca^+(H_2O)_4$	**4-1** → **4-2**	10.42	16.35	13.92	−13.17	17.85
$Ca^+(H_2O)_5$	**5-2** → **5-1**	12.47	12.17	11.32	−2.85	12.17
	5-2 → **5-3**	30.19	38.29	34.42	−30.07	43.38
$Ca^+(H_2O)_6$	**6-4** → **6-2**	5.47	3.33	3.72	−7.92	6.09
	6-4 → **6-3**	6.00	3.95	4.60	2.23	3.93
	6-4 → **6-1**	17.53	13.62	13.96	1.02	13.65
$Ca^+(H_2O)_7$	**7-3** → **7-2**	−0.07	2.08	0.21	−27.16	8.31
	7-3 → **7-1**	1.67	0.53	−0.74	−22.08	5.84
$Ca^+(H_2O)_8$	**8-2** → **8-1**	7.38	4.30	5.42	13.51	1.40
	8-2 → **8-3**	18.28	15.87	18.41	35.25	7.90

[a] Energy differences ΔE_{iso} (kJ/mol) are evaluated with and without zero-point vibrational correction. Enthalpy change ΔH_{iso} (kJ/mol), entropy change ΔS_{iso} (J/mol K), with Gibbs' free energy change ΔG_{iso} (kJ/mol) are evaluated at room temperature (298.15 K).

Two types of isomers are found for $Ca^+(H_2O)_3$, and the structures are **3-1** and **3-2** in Figure 1. The most stable isomer of $Ca^+(H_2O)_3$ is structure **3-1**, in which all three water molecules are directly bonded to the Ca^+ ion. The O−Ca−O angle in $Ca^+(H_2O)_3$ (structure **3-1**) are 120°, and, thus, three oxygen atoms and the calcium ion lie on a plane. The isomer **3-1** belongs to the D_{3h} point group. The second conformer of $Ca^+(H_2O)_3$ is structure **3-2**, which has a second hydration shell. The water molecule of the second shell forms a six-membered ring with two first-shell water molecules and the metal ion. In the most stable isomer of $Mg^+(H_2O)_3$ the three water molecules

TABLE 2: Thermochemical Functions for Hydration Reaction of $Ca^+(H_2O)_n$ and $CaOH^+(H_2O)_n$[a]

reaction	$-\Delta E_{hyd}$	$-\Delta H_{hyd}$	ΔS_{hyd}	$-\Delta G_{hyd}$
$2H_2O \rightarrow (H_2O)_2$	23.53	16.21	−82.2	−8.30
$Ca^+ + H_2O \rightarrow Ca^+(H_2O)$	112.19	123.50	−118.2	88.25
$Ca^+(H_2O) + H_2O \rightarrow Ca^+(H_2O)_2$	105.77	106.19	−96.9	77.28
$Ca^+(H_2O)_2 + H_2O \rightarrow Ca^+(H_2O)_3$ (**3-1**)	81.68	84.15	−125.7	46.12
$Ca^+(H_2O)_3$ (**3-1**) $+ H_2O \rightarrow Ca^+(H_2O)_4$ (**4-1**)	68.40	69.22	−117.6	34.15
$Ca^+(H_2O)_4$ (**4-1**) $+ H_2O \rightarrow Ca^+(H_2O)_5$ (**5-2**)	53.18	55.83	−121.8	19.52
$Ca^+(H_2O)_5$ (**5-2**) $+ H_2O \rightarrow Ca^+(H_2O)_6$ (**6-4**)	46.07	49.56	−135.3	9.23
$Ca^+(H_2O)_6$ (**6-4**) $+ H_2O \rightarrow Ca^+(H_2O)_7$ (**7-3**)	42.13	44.77	−137.0	3.93
$Ca^+(H_2O)_7$ (**7-3**) $+ H_2O \rightarrow Ca^+(H_2O)_8$ (**8-2**)	46.90	50.92	−154.2	4.94
	$-\Delta E'_{hyd}$	$-\Delta H'_{hyd}$	$\Delta S'_{hyd}$	$-\Delta G'_{hyd}$
$CaOH^+ + H_2O \rightarrow CaOH^+(H_2O)$	141.27	145.10	−103.5	114.23
$CaOH^+(H_2O) + H_2O \rightarrow CaOH^+(H_2O)_2$	129.55	130.88	−108.8	98.45
$CaOH^+(H_2O)_2 + H_2O \rightarrow CaOH^+(H_2O)_3$	117.23	118.89	−117.0	84.00
$CaOH^+(H_2O)_3 + H_2O \rightarrow CaOH^+(H_2O)_4$	97.08	99.55	−139.3	58.02
$CaOH^+(H_2O)_4 + H_2O \rightarrow CaOH^+(H_2O)_5$	79.61	83.34	−151.0	38.32
$CaOH^+(H_2O)_5 + H_2O \rightarrow CaOH^+(H_2O)_6$	54.60	57.90	−136.1	17.30
$CaOH^+(H_2O)_6 + H_2O \rightarrow CaOH^+(H_2O)_7$	42.97	44.11	−107.1	12.19

[a] Energy differences ΔE_{iso} and $\Delta E'_{hyd}$ (kJ/mol) are corrected with zero-point vibrational energy. Enthalpy change ΔH_{iso}, $\Delta H'_{hyd}$ (kJ/mol), entropy change ΔS_{iso}, $\Delta S'_{hyd}$ (J/mol K), and Gibbs' free energy change ΔG_{iso}, $\Delta G'_{hyd}$ (kJ/mol) are evaluated at room temperature (298.15 K). Functions with prime are those to the hydrogen-eliminated clusters $CaOH^+(H_2O)_n$.

are also directly coordinated to the metal ion, but in contrast to the planarity of the Ca^+ ions and three oxygens in structure **3-1**, the corresponding four atoms in the most stable $Mg^+(H_2O)_3$ form a pyramidal structure.

In Table 1, energy differences (ΔE_{iso}) are given both with and without zero-point vibration energy correction. Enthalpy (ΔH_{iso}), entropy (ΔS_{iso}), and Gibbs' free energy changes (ΔG_{iso}) are evaluated at room temperature (298.15 K). Needless to say, the energy differences ΔE_{iso} with zero-point vibration energy correlation coincide with ΔH_{iso} and ΔG_{iso} at 0 K under the ideal gas assumption. Of the two isomers of $Ca^+(H_2O)_3$, structure **3-2** is 33.96 kJ/mol less stable than structure **3-1**. The enthalpy change ΔH_{iso} is 30.89 kJ/mol and is almost equal to ΔE_{iso} with zero-point vibrational energy correction. The entropy change ΔS_{iso} of reaction **3-1** to **3-2** is −28.09 kJ/mol K. Because of the rigidity of the six-membered ring in **3-2**, entropy is reduced by the isomerization **3-1** to **3-2**.

Structure **4-1** is the most stable structure of $Ca^+(H_2O)_4$. All four water molecules are directly bonded to the Ca^+ ion. The O−Ca−O angle is close to 90°. The cluster $Ca^+(H_2O)_4$ (**4-1**) belongs to the C_s point group, slightly deformed from the D_{2h} point group. In structure **4-2** of $Ca^+(H_2O)_4$, only three water molecules are directly bonded to the Ca^+ ion. Isomer **4-2** has a six-membered ring, similarly to **3-2**, and it is 16.35 kJ/mol less stable than structure **4-1**.

The optimized structures of the $Ca^+(H_2O)_5$ clusters are shown in Figure 2. Here we found three stable structures. In structure **5-1**, all five water molecules are directly bonded to the Ca^+ ion. Four water molecules form a deformed square, and the remaining water is bound to the calcium ion nearly vertically to this plane. Structure **5-2** is the most stable among the three isomers found for $Ca^+(H_2O)_5$. Four water molecules form the first solvation shell, and the fifth water is in the second shell. The fifth water molecule forms a six-membered ring with the first shell waters similar to structure **3-2** and **4-2**. In the case of isomer **5-2**, the stable six-membered ring can be formed without loosing the approximate planarity. Structure **5-3** has three water molecules in the first shell. The water molecules of the second hydration shell form two kinds of ring structures by hydrogen bonding to the first-shell waters. One ring is a six-membered ring similar to that in **4-2**, and the others are two larger eight-membered rings. Structure similar to **5-3** of $Ca^+(H_2O)_5$ was found for $Mg^+(H_2O)_5$[17] and $Al^+(H_2O)_5$.[27,28] Structure **5-2** is the most unstable among the three isomers. On

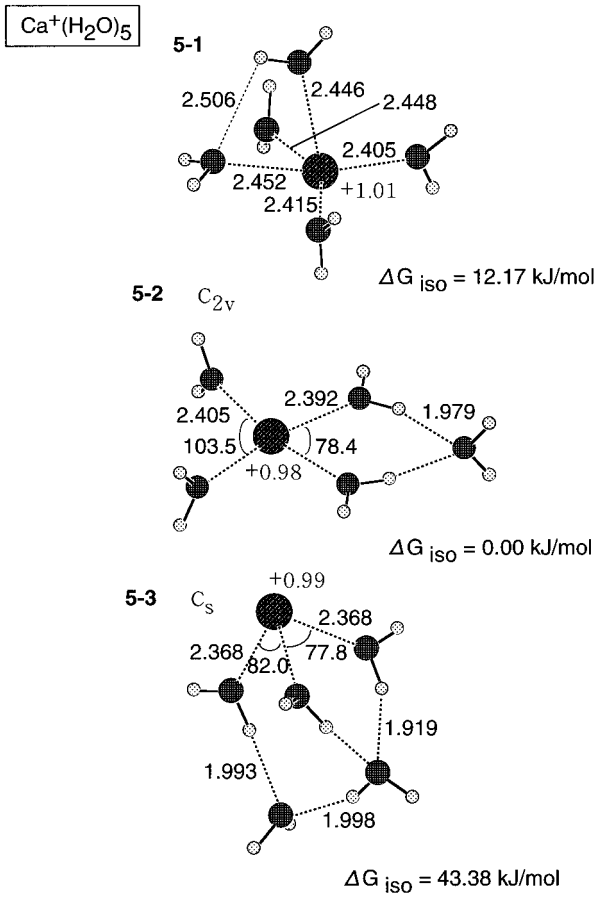

Figure 2. Geometric structures of $Ca^+(H_2O)_5$.

the contrary, for $Mg^+(H_2O)_5$ and $Al^+(H_2O)_5$, the structure similar to **5-3** is the most stable one. In $Mg^+(H_2O)_5$ and $Al^+(H_2O)_5$, the cluster is stabilized by the hydrogen bondings. In contrast, in $Ca^+(H_2O)_5$, the hydrogen-bond network cannot compensate for the loss of the stable square structure. The entropy reduction ΔS_{iso} for the isomerization from **5-2** to **5-3** is large because of more hydrogen bondings in the latter. Thus, Gibbs' free energy change ΔG_{iso} at room temperature of the reaction **5-2** to **5-3** is much larger than ΔG_{iso} for **5-2** to **5-1**.

The optimized structures of $Ca^+(H_2O)_6$, $Ca^+(H_2O)_7$, and $Ca^+(H_2O)_8$, are shown in Figures 3−5, respectively. In these larger clusters, the hydrogen-bonding network is partially formed

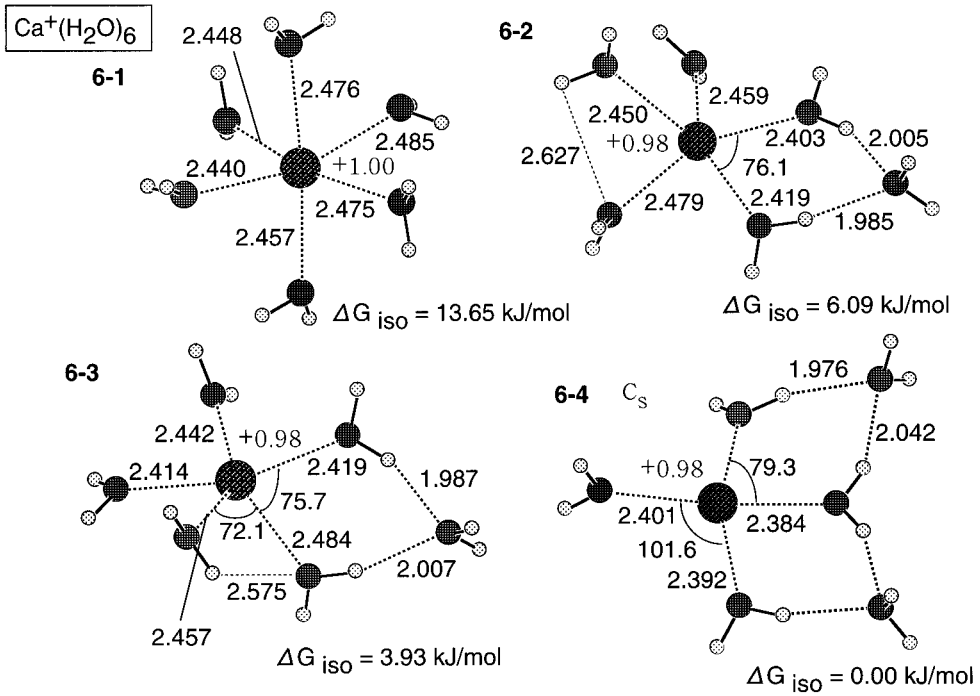

Figure 3. Geometric structures of $Ca^+(H_2O)_6$.

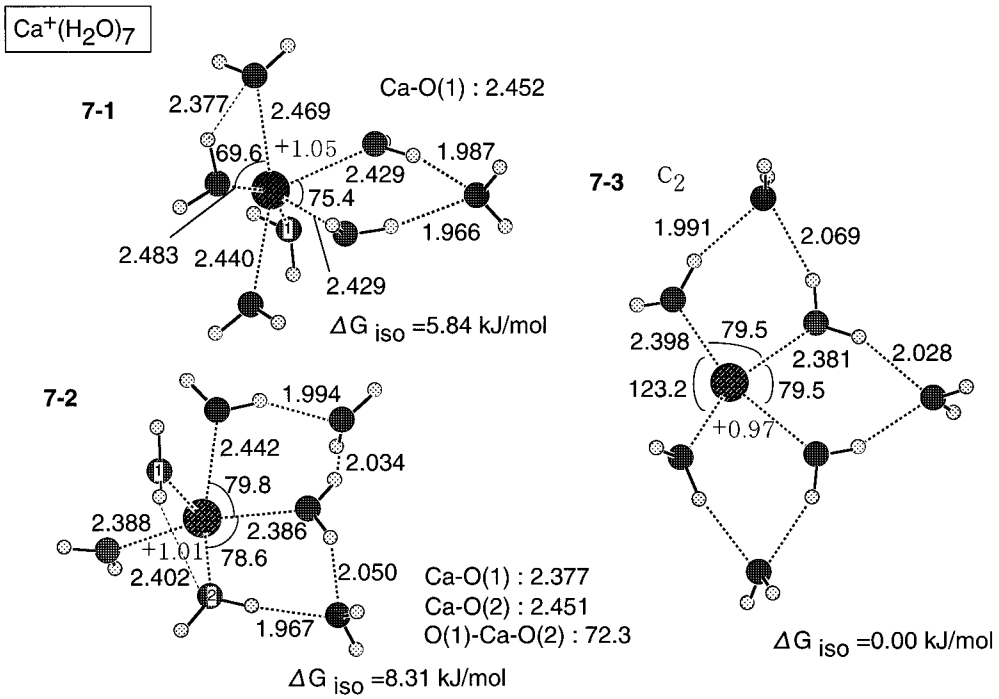

Figure 4. Geometric structures of $Ca^+(H_2O)_7$.

among the water molecules. The most stable isomers are structure **6-4** for $Ca^+(H_2O)_6$ and structure **7-3** for $Ca^+(H_2O)_7$. The hydration number of the most stable isomers of $Ca^+(H_2O)_6$ and $Ca^+(H_2O)_7$ is four, and the planarity of a metal and four oxygens is slightly deformed. The energy differences among these isomers are, however, very small. The second and third stable isomers of $Ca^+(H_2O)_6$ are structures **6-2** and **6-3**, respectively, whose hydration numbers are five. The energy difference between **6-2** and **6-3** after the zero-point vibration energy correction is almost zero. The isomer of $Ca^+(H_2O)_6$ in which six water molecules are in the first shell (structure **6-1**) is much less stable than the others. The energy difference ΔE_{iso} among the three isomers of $Ca^+(H_2O)_7$ is very small. The entropy factor, however, favors **7-3**, due to the hydrogen-bond network. Isomers **7-1** and **7-3** will become less stable in higher temperature, but the instability is still not so significant at room temperature. Among the $Ca^+(H_2O)_8$ isomers, the most stable isomer corresponds structure **8-2**, in which five water molecules are in the first shell. But at the room temperature, the Gibb's free energy of **8-1** is close to that of **8- 2**. Under higher temperature conditions, the dominant cluster $Ca^+(H_2O)_8$ may have six water molecules in the first shell. Although structure **8-3** is highly symmetric (C_{4v}), the entropy change for isomerization **8-2** to **8-3** is a large positive value.

3.1.1. Comparison of Hydrated Singly Charged Typical Elements Clusters. For $n = 1$, the structures of $Ca^+(H_2O)$ and $Mg^+(H_2O)$ are very similar to each other. On the other hand, for $n \geq 2$, the structures of $Ca^+(H_2O)_n$ and $Mg^+(H_2O)_n$ are

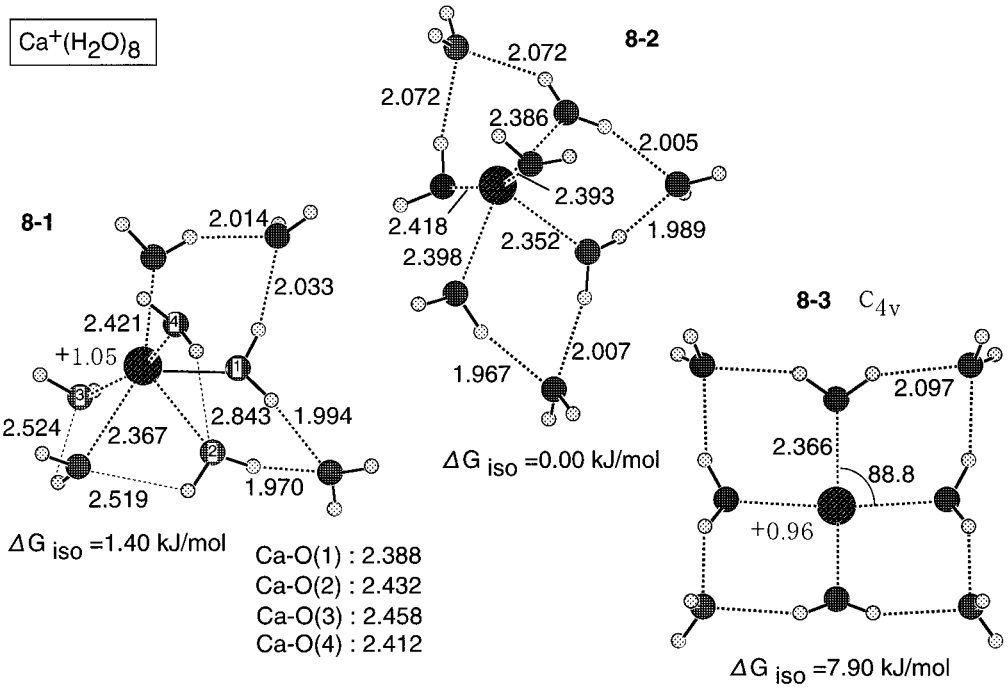

Figure 5. Geometric structures of $Ca^+(H_2O)_8$.

different. The angles of O−Mg−O are almost 90° in the clusters $Mg^+(H_2O)_2$ and $Mg^+(H_2O)_3$.[13,16,17] In contrast, O−Ca−O in $Ca^+(H_2O)_2$ is collinear, and Ca^+-O_3 of $Ca^+(H_2O)_3$ are in a plane. In $Mg^+(H_2O)_n$, the angles of O−Mg−O always keep close to 90° at least up to $n = 6$. Bauschlicher explained the small angle by the sp^3 hybridization of Mg^+. The nonbonding orbital of waters is directed toward the vacant sp^3 hybrid orbitals of Mg^+.[13] Water molecules in the first shell are bound at one side of the Mg^+ ion, and they avoid an odd electron distributed in the other side of the central metal ion; an odd electron of Mg^+ occupies one of four sp^3 hybrid orbitals; the remaining three hybrid orbitals are coordinated by the nonbonding orbitals of oxygen. The hydration structure similar to $Mg^+(H_2O)_n$ is a "surface" type as named by Hashimoto et al.[29,30] The structures of $Al^+(H_2O)_n$ and $B^+(H_2O)_n$ are also surface type clusters which are explained by the repulsive interaction between the water molecules and the lone pair electrons occupied in one of sp^3 orbital of Al^+ and B^+.[16,27,28] In contrast, the structures of the singly charged $Na^+(H_2O)_n$ and $Li^+(H_2O)_n$ are not of surface type, because they have neither the odd electron nor lone-pair electrons;[29,31−33] the electrostatic interaction among the charge and the dipoles determines the shell of the clusters. For $n \geq 3$, the stable local minima having six-membered rings were also found for Na^+−water and Li^+−water clusters but they are not the most stable isomers. Clusters of $Na^+(H_2O)_n$ and $Li^+(H_2O)_n$ have planar structures.

The first shell of $Ca^+(H_2O)_n$ forms a square-planar or a octahedral structure slightly deformed by the second hydration and the hydrogen-bond network. The hydration structure of $Ca^+(H_2O)_n$ is named the "interior" by Hashimoto et al.[29,30] The reason for the structural difference between $Mg^+(H_2O)_n$ and $Ca^+(H_2O)_n$ is 2-fold. As mentioned above, the odd electron (or SOMO) in $Mg^+(H_2O)_n$ is localized on a sp^3 hybrid orbital located opposite from water molecules. By contrast, in $Ca^+(H_2O)_n$, the SOMO is a spherical 4s orbital. The natural electron population of 4s ranges from 0.98 ($n = 1$) to 0.86 ($n = 4$), and the remaining occupation on the Ca^+ ion is not on the 4p orbital, but on the 3d orbital; the population of 3d is 0.03 for $n = 1$ and 0.15 for $n = 4$. Consequently these d orbitals of Ca^+ cause the structural differences compared to the

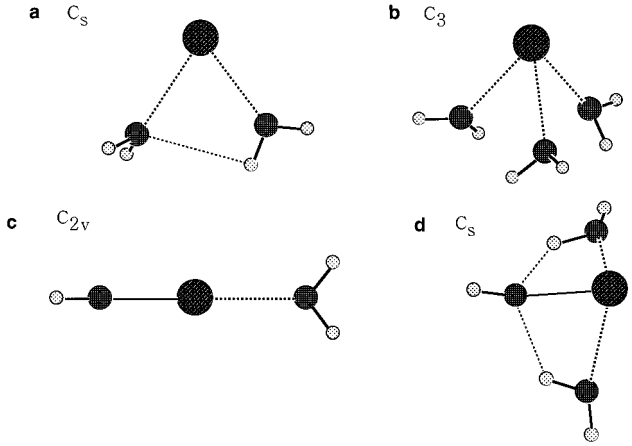

Figure 6. Optimized structures of $Ca^+(H_2O)_n$ and $CaOH^+(H_2O)_{n-1}$ for $n = 2$ and 3 without d basis functions on a calcium atom. (**a**) $Ca^+(H_2O)_2$; (**b**) $Ca^+(H_2O)_3$; (**c**) $CaOH^+(H_2O)$; (**d**) $CaOH^+(H_2O)_2$.

$Mg^+(H_2O)_n$ clusters. Figure 6 shows the structures of $Ca^+(H_2O)_2$ (**a**) and $Ca^+(H_2O)_3$ (**b**) optimized by excluding all of the d basis functions of the calcium atom. Structures **a** and **b** are surface clusters very similar to those of $Mg^+(H_2O)_n$. In particular, two water molecules are bound with hydrogen bonding in structure **a**, which is also seen in neutral $Na(H_2O)_2$.[30,34]

The most stable isomers of $Mg^+(H_2O)_4$, $Al^+(H_2O)_4$ and $B^+(H_2O)_4$ have a six-membered rings,[16,27,28] which contributes to the stabilization of these clusters. On the other hand, in $Ca^+(H_2O)_4$, a quasi-square structure is favored, and structure **4-2** with a six-membered ring is less stable.

3.2. Structures of Hydrogen-Eliminated Clusters $CaOH^+(H_2O)_{n-1}$. The optimized structures of the hydrogen eliminated clusters $CaOH^+(H_2O)_{n-1}$ are shown in Figure 7. As in $MgOH^+(H_2O)_n$, a $CaOH^+$ builds the core of the $CaOH^+$-$(H_2O)_n$ cluster. The charge distribution of the molecular ion $CaOH^+$ is strongly polarized, and the calcium ion is oxidized to almost +2. The binding energy between $CaOH^+$ and water is, therefore, larger than for the Ca^+ ion. The strong electrostatic bond is the determining factor for the geometric structures, and thus, the most stable isomer of $CaOH^+(H_2O)_n$ has five water

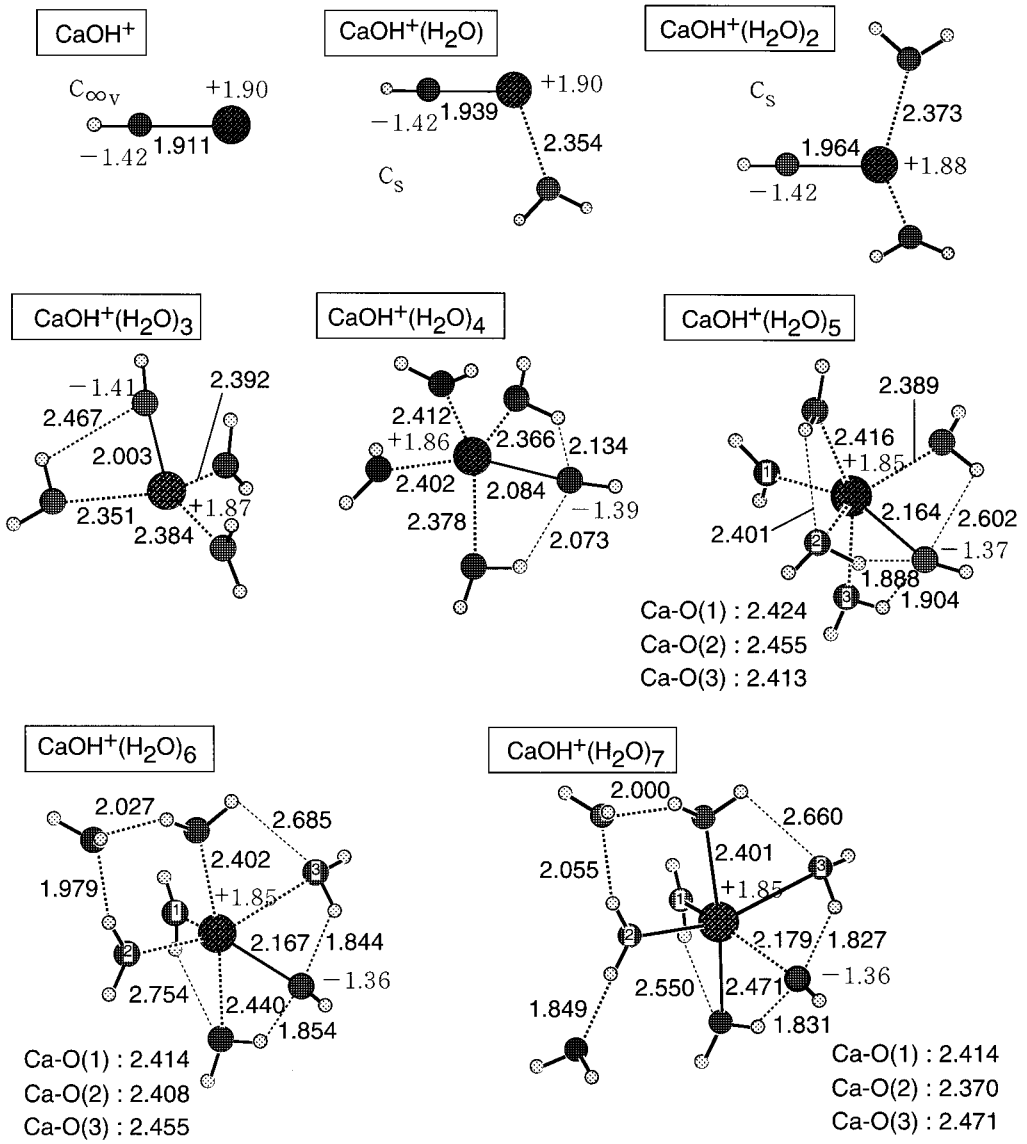

Figure 7. Geometric structures of hydrogen eliminated clusters $CaOH^+(H_2O)_{n-1}$.

molecules in the first shell. The clusters $CaOH^+(H_2O)_6$ and $CaOH^+(H_2O)_7$ have second hydration water molecules. Moreover, for $n \geq 4$, a hydrogen-bond network among water molecules and the OH moiety is formed in the clusters. In particular, a strongly negative charged oxygen of $CaOH^+$ attracts the hydrogen atom(s) of the water molecule(s).

Unlike the water clusters of Mg^+ and Ca^+ ions, the water clusters of $MgOH^+$ and $CaOH^+$ have common character, because the electrostatic interaction is the most important.[1,17] A similar polarized molecular ion is found for $HAlOH^+$. In the molecular ion $HAlOH^+$, aluminum is oxidized and it becomes near $HAl^{2+}OH^-$.[28]

The structures of bare $CaOH^+$ ion and $MgOH^+$ ion are both linear. In contrast, a large structural difference is found between $CaOH^+(H_2O)_{n-1}$ and $MgOH^+(H_2O)_{n-1}$ for $n \geq 2$. The cluster $MgOH^+(H_2O)$ has a linear backbone structure.[11,17] On the other hand, $CaOH^+(H_2O)$ is bent. The structural difference in $CaOH^+(H_2O)$ and $MgOH^+(H_2O)$ is again due to the participation of d orbitals in $CaOH^+$. The structures of $CaOH^+(H_2O)$ and $CaOH^+(H_2O)_2$ determined without d type basis functions on the calcium atom is shown in Figure 6 (**c** and **d**), which clearly demonstrates the important role of d functions. Structure **c** is linear and similar to $MgOH^+(H_2O)$, while structure **d** is different both from that of $MgOH^+(H_2O)_2$ and from that determined with d functions for $CaOH^+(H_2O)_2$. In structure **d**, two water molecules are bonded to oxygen of $CaOH^+$.

3.3. Product Switch of the Reaction $Ca^+(H_2O)_n$. To elucidate the observed product switch in the reaction of the Ca^+ ion and water clusters, we have drawn the energy diagram of the hydration and hydrogen elimination energies of $Ca^+(H_2O)_n$ in Figure 8. The hydration energies are evaluated for the following reactions:

$$Ca^+(H_2O)_{n-1} + H_2O \rightarrow Ca^+(H_2O)_n \quad (2)$$

$$CaOH^+(H_2O)_{n-1} + H_2O \rightarrow CaOH^+(H_2O)_n \quad (3)$$

The incremental hydrogen elimination reaction is

$$Ca^+(H_2O)_n \rightarrow (CaOH)^+(H_2O)_{n-1} + H \quad (4)$$

The incremental hydration energies of $Ca^+(H_2O)_n$ ($\Delta E_{hyd}(n)$) and $CaOH^+(H_2O)_n$ ($\Delta E'_{hyd}(n)$), are defined by

$$\Delta E_{hyd}(n) = E(n) - [E(n-1) + E(H_2O)] \quad (5)$$

$$\Delta E'_{hyd}(n) = E'(n) - [E'(n-1) + E(H_2O)] \quad (6)$$

where $E(n)$ and $E'(n)$ are the total energies of $Ca^+(H_2O)_n$ and

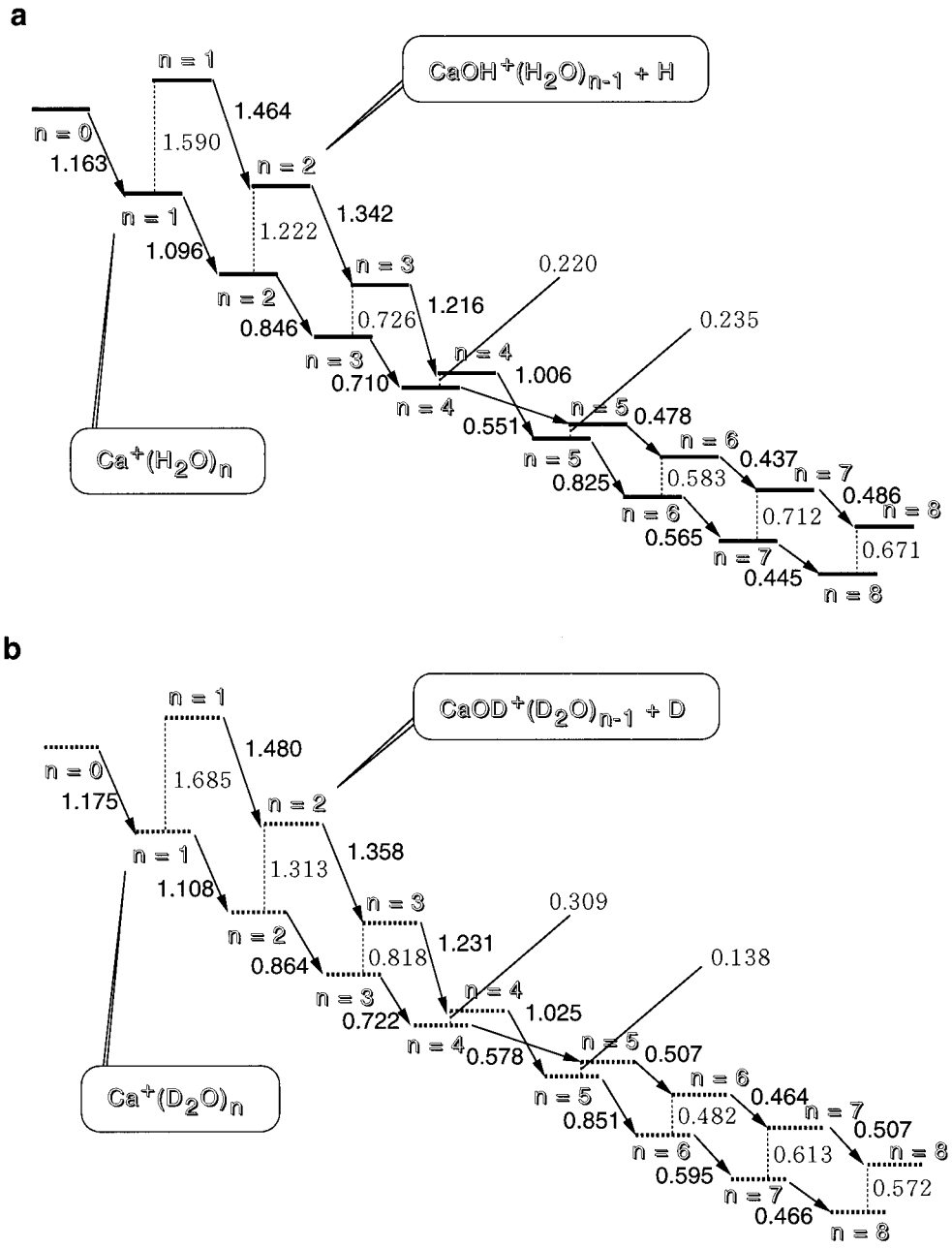

Figure 8. Hydration and reaction energies (/eV) of $Ca^+(H_2O)_n$ (**a**) and $Ca^+(D_2O)_n$ (**b**) with the zero-point vibrational correction. The vertical dotted lines are the hydrogen (deuterium) elimination reaction energies of $Ca^+(H_2O)_n$ $\Delta E_{elm}(n)$ ($Ca^+(D_2O)_n$ $\Delta E_{D,elm}(n)$). The arrows are the hydration energies of the ions.

$CaOH^+(H_2O)_{n-1}$, respectively, and $E(H_2O)$ is the total energy of a free water molecule. The hydrogen eliminated energy is defined as

$$\Delta E_{elm}(n) = [E'(n-1) + E(H)] - E(n) \qquad (7)$$

where $E(H)$ is the total energy of hydrogen atom.

The energy diagram of the $Ca^+(H_2O)_n$ system is very similar to the corresponding diagram of the $Mg^+(H_2O)_n$ system.[17] The diagonal arrows in Figure 8**a** are hydration energies of $Ca^+(H_2O)_n$ ($\Delta E_{hyd}(n)$) and $CaOH^+(H_2O)_{n-1}$ ($\Delta E'_{hyd}(n)$) for reactions 2 and 3, and the dotted vertical lines are the hydrogen-elimination energies of $Ca^+(H_2O)_n$ ($\Delta E_{elm}(n)$) for reaction 4. Both hydration and hydrogen-elimination energies include the zero-point vibration energy corrections. Because of strong polarization of the molecular ion $CaOH^+$, the hydration energies of $CaOH^+(H_2O)_{n-1}$ ($\Delta E'_{hyd}(n)$) is larger than that of $Ca^+(H_2O)_n$ ($\Delta E_{hyd}(n)$) clusters. For $n = 1$, the hydrogen-elimination energy $\Delta E_{elm}(1)$ is positive and large. Eventually $\Delta E_{elm}(n)$ becomes negative for $n \geq 5$. The stability of $CaOH^+(H_2O)_{n-1} + H$ and $Ca^+(H_2O)_n$ reverses in $n \geq 5$. Thus, the first product switch found by Fuke's group can be explained qualitatively with this internal energy diagram. In the case of $Mg^+(H_2O)_n$ system, the calculated energy of $\Delta E^{(Mg)}_{elm}(1)$ is 2.90 eV using the MP2(frozen core)//SCF level of approximation,[17] which is almost twice of $\Delta E_{elm}(1)$ (=1.59 eV) of $Ca^+(H_2O)$. The calculated hydrogen eliminated energy $\Delta E^{(Mg)}_{elm}(n)$ becomes negative at $n = 5$. The trends in $Mg^+(H_2O)_n$ and $Ca^+(H_2O)_n$ systems are very similar to each other.

3.3.1. Thermodynamical Functions. Table 2 shows the hydration energy with zero-point vibrational correction $\Delta E_{hyd}(n)$ and several thermochemical functions (enthalpy change $\Delta H_{hyd}(n)$, entropy change $\Delta S_{hyd}(n)$, and Gibbs' free energy change $\Delta G_{hyd}(n)$) at room temperature ($T = 298.15$ K). Thermochemical functions with a prime $\Delta E'_{hyd}(n)$, $\Delta H'_{hyd}(n)$, $\Delta S'_{hyd}(n)$, and

TABLE 3: Thermochemical Functions for Hydrogen-Elimination Reaction of $Ca^+(H_2O)_n$[a]

reaction	ΔE_{elm}	ΔH_{elm}	ΔS_{elm}	ΔG_{elm}
$Ca^+(H_2O) \rightarrow CaOH^+ + H$	153.38	166.12	114.9	131.89
$Ca^+(H_2O)_2 \rightarrow CaOH^+(H_2O) + H$	117.89	127.21	108.2	94.94
$Ca^+(H_2O)_3$ (**3-1**) $\rightarrow CaOH^+(H_2O)_2 + H$	70.02	80.47	127.0	42.61
$Ca^+(H_2O)_4$ (**4-1**) $\rightarrow CaOH^+(H_2O)_3 + H$	21.19	30.81	127.6	−7.24
$Ca^+(H_2O)_5$ (**5-2**) $\rightarrow CaOH^+(H_2O)_4 + H$	−22.70	−12.92	110.1	−45.74
$Ca^+(H_2O)_6$ (**6-4**) $\rightarrow CaOH^+(H_2O)_5 + H$	−56.24	−46.70	94.3	−74.82
$Ca^+(H_2O)_7$ (**7-3**) $\rightarrow CaOH^+(H_2O)_6 + H$	−68.72	−59.83	95.1	−88.20
$Ca^+(H_2O)_8$ (**8-2**) $\rightarrow CaOH^+(H_2O)_7 + H$	−64.78	−53.03	142.3	−95.45

[a] Energy difference ΔE_{iso} (kJ/mol) is evaluated with zero-point vibrational correction. Enthalpy change ΔH_{iso} (kJ/mol), entropy change ΔS_{iso} (J/mol K), and Gibbs' free energy change ΔG_{iso} (kJ/mol) are evaluated at room temperature (298.15 K).

$\Delta G'_{hyd}(n)$ are those for the hydrogen-eliminated clusters $CaOH^+(H_2O)_{n-1}$. After the second hydration starts to form, the energy differences $\Delta E_{hyd}(n)$ and enthalpy change at room temperature $\Delta H_{hyd}(n)$ converge. But, even at $n = 8$, both $-\Delta E_{hyd}(n)$ and $-\Delta H_{hyd}(n)$ are much larger than the dimerization energy of water molecules (−23.53 kJ/mol). On the other hand, entropy reduction $-\Delta S_{hyd}(n)$ becomes larger with cluster size n. One exception is $-\Delta S'_{hyd}(7)$, for $CaOH^+(H_2O)_7$, in which one of the water molecules of the second hydration shell has only one hydrogen bond and therefore moves almost freely (see also Figure 7). Gibbs' free energy changes at room temperature $-\Delta G_{hyd}(n)$ decreases with cluster size, but for $n = 8$, it is still positive. Interestingly, the calculated $-\Delta G$ value for the dimerization of water molecules is negative at room temperature. The n dependence of $-\Delta H_{hyd}(n)$ and $-\Delta S_{hyd}(n)$ suggests that Gibbs' free energy change $-\Delta G_{hyd}(n)$ might eventually become negative for large clusters. In other words, some of the water molecules must be vaporized, if room temperature of the cluster is assumed. In the TOF mass spectra, the clusters of $Ca^+(H_2O)_n$ are found for $15 \leq n \leq 20$.[3] Thus, this may imply that the internal temperature is much lower than room temperature.

Table 3 summarizes the thermochemical functions of hydrogen elimination reactions. Entropy change of hydrogen elimination $\Delta S_{elm}(n)$ is not much dependent of the cluster size n. One exception is again $\Delta S_{elm}(7)$, because of the above-mentioned very weak bonding of one of the second shell waters. The change of the sign in Gibbs's free energy at $n = 4$ ($-\Delta G_{elm}(4)$) is clearly seen in the table. Gibbs' free energy change $-\Delta G_{elm}(4)$ is negative at room temperature, but it becomes positive in lower temperature. In the TOF mass spectra, the dominant cluster for $n = 4$ is $Ca^+(H_2O)_4$, but $CaOH^+(H_2O)_3$ is certainly observed in the TOF spectra.[3] The experimental observation can be explained qualitatively with the calculated Gibbs' free energy change.

3.3.2. Deuterium Replacement Effect. Fuke's group has also investigated the deuterium replacement effect in the product switch. Figure 8**b** is the energy diagram for deuterium replaced cluster $Ca^+(D_2O)_n$ system. Because the number of OH (OD) bonds in $CaOH^+(H_2O)_{n-1}$ ($CaOD^+(D_2O)_{n-1}$) is by one less than that of $Ca(H_2O)_n$($Ca(D_2O)_n$), the reduction of the zero-point vibrational energy of $CaOH^+(H_2O)_{n-1}$ to $CaOD^+(D_2O)_{n-1}$ is larger than that of $Ca^+(H_2O)_n$ to $Ca^+(D_2O)_n$. Hence, the deuterium elimination energies $-\Delta E_{D,elm}(n)$ is larger than the hydrogen-elimination energies $-\Delta E_{H,elm}(n)$ in every cluster size n. The first product switch takes place at $n = 6$ in $Ca^+(D_2O)_n$ and at $n = 5$ in $Ca^+(H_2O)_n$. The deuterium replacement effect on the product distribution can be explained with the thermochemical stability.

3.3.3. Equilibrium Constants of the Hydrogen-Elimination Energies. Equilibrium constants of hydrogen (deuterium) elimination reactions are evaluated to clarify the size, temperature, and isotope dependence of the $Ca^+(H_2O)_n$ system more quantitatively. Figure 9 shows logarithmic plots of the equilibrium constants, $\log K_p(n)$ and $\log K_{p,D}(n)$, against reciprocal of temperature ($1/T$) for the clusters $3 \leq n \leq 6$. Equilibrium constants $K_p(n)$ and $K_{p,D}(n)$ are defined by

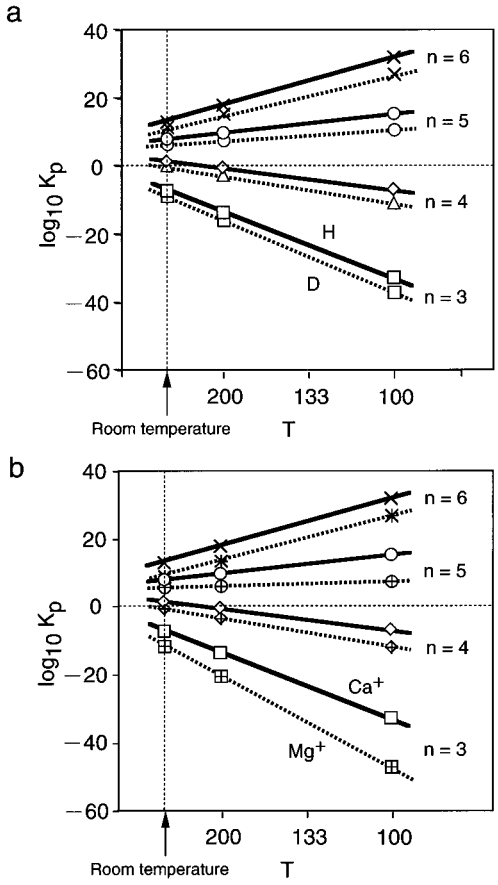

Figure 9. Logarithmic plots of the equilibrium constants $K_p(n)$ ($K_{p,D}$) of hydrogen (deuterium) elimination reaction. (**a**) $Ca^+(H_2O)_n$ and $Ca^+(D_2O)_n$; (**b**) $Ca^+(H_2O)_n$ and $Mg^+(H_2O)_n$.

$$Ca^+(H_2O)_n \rightarrow (CaOH)^+(H_2O)_{n-1} + H \qquad (4)$$

$$Ca^+(D_2O)_n \rightarrow (CaOD)^+(D_2O)_{n-1} + D \qquad (8)$$

The assumed gas pressure is 1.0 atm. The dissociation products, $CaOH^+(H_2O)_{n-1} + H$ or $CaOD^+(D_2O)_{n-1} + D$, are dominant in the region of $\log K_p(n) > 0$ ($K_p(n) \geq 1$). Because of the sign change of ΔE_{elm} and $\Delta E_{D,elm}$, the slope of the $\log K_p(n)$ against $1/T$ becomes positive in $n \geq 5$. For any cluster size n, the equilibrium constants of reaction 4 (for light hydrogen) are larger than reaction 8 (for deuterium). In the experiment,[3] the equilibrium moves to dissociation products, when hydrogens are replaced by deuteriums, which is consistent with our calculated isotope effect.

For $n = 4$, the logarithmic of the equilibrium constant, $\log K_p(n)$, is positive at room temperature but becomes negative at the lower temperature. As mentioned in the previous paragraph, the product distribution of $Ca^+(H_2O)_4$ in the experiments can be explained by assuming a lower temperature range. But in the case of $Ca^+(D_2O)_5$ and $Ca^+(D_2O)_6$, the calculated equilibrium constants $\log K_{p,D}(5)$ and $\log K_{p,D}(6)$ are always positive in the temperature region in Figure 9**a**, while in the experimental TOF spectra, the masses of the reaction products are also detected. This apparent discrepancy might be due to the thermochemical equilibrium assumption in the theoretical evalu-

TABLE 4: Reaction Energies of Small Ca^+−Water Systems with the MP2(all electrons//SCF and the MP4SDTQ(all electrons) Approximations[a]

reaction	SCF	MP2(all electrons)//SCF	MP4(all electrons)//SCF	experiment
$Ca^+ + H_2O \rightarrow Ca^+(H_2O)$	−112.19	−125.79	−124.48	
$Ca^+(H_2O) + H_2O \rightarrow Ca^+(H_2O)_2$	−105.77	−121.35	−120.88	
$Ca^+(H_2O)_2 + H_2O \rightarrow Ca^+(H_2O)_3$ (**3-1**)	−81.68	−99.98		
$Ca^+(H_2O)_3$ (**3-1**) $+ H_2O \rightarrow Ca^+(H_2O)_4$ (**4-1**)	−68.40	−84.00		
$CaOH^+ + H_2O \rightarrow CaOH^+(H_2O)$	−141.27	−153.38	−151.25	
$CaOH^+(H_2O) + H_2O \rightarrow CaOH^+(H_2O)_2$	−129.55	−143.51		
$CaOH^+(H_2O)_2 + H_2O \rightarrow CaOH^+(H_2O)_3$	−117.23	−132.84		
$Ca^+(H_2O) \rightarrow CaOH^+ + H$	153.38	136.18	140.14	167
$Ca^+(H_2O)_2 \rightarrow CaOH^+(H_2O) + H$	117.89	104.16	109.77	
$Ca^+(H_2O)_3 \rightarrow CaOH^+(H_2O)_2 + H$	70.02	60.63		
$Ca^+(H_2O)_4 \rightarrow CaOH^+(H_2O)_3 + H$	21.19	11.79		
$CaOH^+(H_2O)_2 \rightarrow CaOH^+ + H_2O + H$	259.15	257.54	261.01	276

[a] Units are given in kJ/mol. The experimental data are from ref 3.

TABLE 5: Hydration Energies without Zero-Point Vibrational Correction of Ca^+ and $CaOH^+$ with and without Basis Set Super Position (BSSE) Error Correction $\Delta E'$ and ΔE[a]

reaction	without BSSE ΔE	with BSSE $\Delta E'$	ratio $(\Delta E'/\Delta E) \times 100\%$
$Ca^+ + H_2O \rightarrow Ca^+(H_2O)$	−118.75	−108.67	91.5
$Ca^+(H_2O) + 2H_2O \rightarrow Ca^+(H_2O)_2$	−231.11	−210.05	90.9
$Ca^+(H_2O) + 3\ H_2O \rightarrow Ca^+(H_2O)_3$ (**3-1**)	−320.89	−284.24	88.6
$Ca^+(H_2O) + 4\ H_2O \rightarrow Ca^+(H_2O)_4$ (**4-1**)	−396.24	−350.91	88.6
$CaOH^+ + H_2O \rightarrow CaOH^+(H_2O)$	−149.35	−137.56	92.1
$CaOH^+(H_2O) + 2\ H_2O \rightarrow CaOH^+(H_2O)_2$	−286.81	−262.83	91.6
$CaOH^+(H_2O) + 3\ H_2O \rightarrow CaOH^+(H_2O)_3$	−412.26	−376.90	91.4
$CaOH^+(H_2O) + 4\ H_2O \rightarrow CaOH^+(H_2O)_4$	−518.59	−483.20	93.2

[a] Units are given in kJ/mol.

ation. Under real experimental conditions, the thermochemical equilibrium is not attained.

To investigate the metal dependence, Figure 9**b** compares the equilibrium constants of $Ca^+(H_2O)_n$ and $Mg^+(H_2O)_n$. According to the experiments, the first product switch of the clusters $Mg^+(H_2O)_n$ takes place at $n = 6$, while for the cluster $Ca^+(H_2O)_n$ system, at $n = 5$. The calculated equilibrium constants ($K_p^{(Mg)}(n)$) are always lower than ($K_p^{(Ca)}(n)$).

3.4. More Accurate Estimation and BSSE Correction. To estimate the electron correlation effect, the hydration and hydrogen-elimination reaction energies for small clusters are calculated using the MP2(all electrons) and MP4SDTQ(all electrons) levels of approximation at the SCF optimized structures. In Table 4, the energies of SCF, MP2, and MP4SDTQ approximations are shown. The experimental data determined by Fuke et al. are also shown in Table 4. The differences between SCF and MP2//SCF are about 10−15 kJ/mol and between MP2//SCF and MP4SDTQ//SCF are very small. There is an electron correlation effect on the hydration and hydrogen-elimination reactions of calcium−water clusters, but it is not significant enough to change the chemistry involved.

There is one problem in directly comparing $K_p^{(Ca)}$ and $K_p^{(Mg)}$ in Figure 9**b**. In the previous study, the hydration energies of $Mg^+(H_2O)_n$ and $MgOH^+(H_2O)_n$ are evaluated with the MP2-(frozen core)//SCF level of approximation.[17] In contrast, the hydration energies of $Ca^+(H_2O)_n$ and $CaOH^+(H_2O)_n$ in the present study are evaluated with the SCF//SCF level of approximation. In both case, the zero-point vibrational energy correction and partition functions are evaluated with the SCF//SCF level of approximation. The SCF level of approximation in $Ca^+(H_2O)_n$ system is, however, sufficient to discuss the reactions quantitatively. Thus, we can safely compare K_p for $Ca^+(H_2O)_n$ and $K_p^{(Mg)}$ for $Mg^+(H_2O)_n$.

Table 5 summarizes the basis set superposition error (BSSE)[35] of reactions 9 and 10 up to $n = 4$.

$$Ca^+ + nH_2O \rightarrow Ca^+(H_2O)_n \qquad (9)$$

$$CaOH^+ + nH_2O \rightarrow CaOH^+(H_2O)_n \qquad (10)$$

In systems of $Ca^+(H_2O)_n$ and $CaOH^+(H_2O)_n$, the reaction energies with BSSE correction ($\Delta E'$) are about 90% of those without correction (ΔE).

4. Conclusion

Because of the participation of the d orbital in the bonding, the structures of $Ca^+(H_2O)_n$ and $CaOH^+(H_2O)_{n-1}$ are quite different from the corresponding structures of $Mg^+(H_2O)_n$ and $MgOH^+(H_2O)_{n-1}$. Despite the structural differences, the trends in the hydrogen-elimination reaction of $Ca^+(H_2O)_n$ are similar to those of $Mg^+(H_2O)_n$. The similarity is attributed to be the strongly polarized product molecular ion $CaOH^+$ and $MgOH^+$. The first product switch of the $Ca^+(H_2O)_n$ system can be explained by thermochemical arguments as it is the case in the $Mg^+(H_2O)_n$ system.

How about the other hydrated singly charged group 2 metal clusters? Their relative stabilities are assumed to be similar to $Ca^+(H_2O)_n$ and $Mg^+(H_2O)_n$. But in the case of $Be^+(H_2O)_n$, it can be expected that the trends of the relative stability are somewhat more complicated. In the previous studies, we investigated the structure and stability of $B^+(H_2O)_n$, and showed complicated stability and reactivity trends due to hybridization effects in boron.[28] The beryllium atom belonging to the second period is also expected to undergo hybridization.

In both $Ca^+(H_2O)_n$ and $Mg^+(H_2O)_n$, the mechanism of the second product switch is not sufficiently rationalized yet. More extensive studies are required to resolve the questions involving the second product switch.

Acknowledgment. The authors thank Prof. Fuke for discussion throughout the research. The authors wish to thank Dr. J. Hrušák and Dr. A. Fiedler for reading the manuscript critically. H.W. thanks Research Fellowships of the Japan Society for the Promotion of Science for Young Scientists for financial support. The work is partially supported by the Grant-in-Aids for

Scientific Research (No. 04640458) and for the Priority Area (No. 04243102) by the Ministry of Education, Science, Sports and Culture, Japan.

References and Notes

(1) Shen, M. H.; Farrar, J. M. *J. Chem. Phys*. **1991**, *94*, 332.

(2) Shen, M. H.; Winniczek, J. W.; Farrar, J. M. *J. Phys. Chem*. **1987**, *91*, 6447.

(3) Sanekata, M.; Misaizu, F.; Fuke, K. *J. Chem. Phys.* **1996**, *104*, 9768.

(4) Scurlock, C. T.; Pullins, S. H.; Reddic, J. E.; Duncan, M. A. *J. Chem. Phys*. **1996**, *104*, 4591.

(5) Fuke, K.; Misaizu, F.; Sanekata, M.; Tsukamoto, K.; Iwata, S. *Z. Phys. D—Atoms, Mol. Clusters* **1993**, *26S*, 180.

(6) Misaizu, F.; Sanekata, M.; Tsukamoto, K.; Fuke, K.; Iwata, S. *J. Phys. Chem*. **1992**, *92*, 8259.

(7) Yeh, C. S.; Willey, K. F.; Robbins, D. L.; Pilgrim, J. S.; Duncan, M. A. *Chem. Phys. Lett*. **1992**, *196*, 233.

(8) Willey, K. F.; Yeh, C. S.; Robbins, D. L.; Pilgrim, J. S.; Duncan, M. A. *J. Chem. Phys.* **1992**, *97*, 8886.

(9) Sanekata, M.; Misaizu, F.; Fuke, K.; Iwata, S.; Hashimoto, K. *J. Am. Chem. Soc*. **1995**, *117*, 747.

(10) Misaizu, F.; Sanekata, M.; Fuke, K.; Iwata, S. *J. Chem. Phys*. **1994**, *100*, 1161.

(11) Harms, A. C.; Khanna, S. N.; Chen, B.; Castleman, Jr., A. W. *J. Chem. Phys*. **1994**, *100*, 3540.

(12) Sodupe, M.; Bauschlicher Jr., C. W.; Partridge, H. *J. Chem. Phys*. **1991**, *95*, 9422.

(13) Bauschlicher Jr., C. W.; Sodupe, M.; Partridge, H. *J. Chem. Phys*. **1992**, *96*, 4453.

(14) Bauschlicher Jr., C. W.; Partridge, H. *Chem. Phys. Lett*. **1991**, *181*, 129.

(15) Bauschlicher Jr., C. W.; Partridge, H. *J. Phys. Chem*. **1991**, *95*, 3946.

(16) Bauschlicher Jr., C. W.; Partridge, H. *J. Phys. Chem*. **1991**, *95*, 9694.

(17) Watanabe, H.; Iwata, S.; Hashimoto, K.; Fuke, K.; Misaizu, F. *J. Am. Chem. Soc*. **1995**, *117*, 755.

(18) Glendening, E. D.; Feller, D. *J. Phys. Chem*. **1996**, *100*, 4790.

(19) Hashimoto, K.; Yoda, N.; Iwata, S. *Chem. Phys*. **1987**, *116*, 193.

(20) Hashimoto, K.; Iwata, S. *J. Phys. Chem*. **1989**, *93*, 2165.

(21) Hashimoto, K.; Yoda, N.; Osamura, Y.; Iwata, S. *J. Am. Chem. Soc*. **1990**, *112*, 7189.

(22) Kochanski, E.; Constantin, E. *J. Chem. Phys*. **1987**, *87*, 1661.

(23) Pettersson, L. G. M.; Siegbahn, P. E. M.; Ismail, S. *Chem. Phys.* **1983**, *82*, 355.

(24) Gaussian 92, Revision E.2; Frisch, M. J.; Trucks, G. W.; Head-Gordon, M.; Gill, P. M. W.; Wong, M. W.; Foresman, J. B.; Johnson, B. G.; Schlegel, H. B.; Robb, M. A.; Replogle, E. S.; Gomperts, R.; Andres, J. L.; Raghavachari, K.; Binkley, J. S.; Gonzalez, C.; Martin, R. L.; Fox, D. J.; Defrees, D. J.; Baker, J.; Stewart, J. J. P.; Pople, J. A. Gaussian, Inc.: Pittsburgh, PA, 1992.

(25) Gaussian 94, Revision B.2; Frisch, M. J.; Trucks, G. W.; Schlegel, H. B.; Gill, P. M. W.; Johnson, B. G.; Robb, M. A.; Cheeseman, J. R.; Keith, T.; Petersson, G. A.; Montgomery, J. A.; Raghavachari, K.; Al-Laham, M. A.; Zakrzewski, V. G.; Ortiz, J. V.; Foresman, J. B.; Cioslowski, J.; Stefanov, B. B.; Nanayakkara, A.; Challacombe, M.; Peng, C. Y.; Ayala, P. Y.; Chen, W.; Wong, M. W.; Andres, J. L.; Replogle, E. S.; Gomperts, R.; Martin, R. L.; Fox, D. J.; Binkley, J. S.; Defrees, D. J.; Baker, J.; Stewart, J. P.; Head-Gordon, M.; Gonzalez, C.; Pople, J. A. Gaussian, Inc.: Pittsburgh, PA, 1995.

(26) E-mail address: iwata@ims.ac.jp.

(27) Watanabe, H.; Aoki, M.; Iwata, S. *Bull. Chem. Soc. Jpn*. **1993**, *66*, 3245.

(28) Watanabe, H.; Iwata, S. *J. Phys. Chem*. **1996**, *100*, 3377.

(29) Hashimoto, K.; Morokuma, K. *Chem. Phys. Lett*. **1994**, *223*, 423.

(30) Hashimoto, K.; Morokuma, K. *J. Am. Chem. Soc*. **1994**, *116*, 11436.

(31) Bauschlicher Jr., C. W.; Langhoff, S. R.; Partridge, H.; Rice, J. E.; Komornicki, A. *J. Chem. Phys*. **1991**, *95*, 5142.

(32) Feller, D.; Glendening, E. D.; Kendall, R. A.; Petersin, K. A. *J. Chem. Phys*. **1994**, *100*, 4981.

(33) Glendening, E. D.; Feller, D. *J. Phys. Chem*. **1995**, *99*, 3060.

(34) Hashimoto, K.; He, S.; Morokuma, K. *Chem. Phys. Lett*. **1993**, *206*, 297.

(35) Boys, S. F.; Bernardi, F. *Mol. Phys*. **1970**, *19*, 553.